

# Measurement of $CP$ Asymmetries and Branching Fractions in $B \rightarrow \pi\pi$ and $B \rightarrow K\pi$ decays.

The *BABAR* Collaboration

July 29, 2006

## Abstract

We present preliminary measurements of the  $CP$  asymmetries and branching fractions for  $B \rightarrow \pi\pi$  and  $B \rightarrow K\pi$  decays. A total of 347 million  $B\bar{B}$  events collected by the *BABAR* detector at the PEP-II asymmetric-energy  $e^+e^-$  collider at SLAC are used for these results. We find

$$\begin{aligned} S_{\pi\pi} &= -0.53 \pm 0.14 \pm 0.02 \\ C_{\pi\pi} &= -0.16 \pm 0.11 \pm 0.03 \\ \mathcal{A}_{K\pi} &= -0.108 \pm 0.024 \pm 0.008 \\ \mathcal{B}(B^0 \rightarrow \pi^0\pi^0) &= (1.48 \pm 0.26 \pm 0.12) \times 10^{-6} \\ \mathcal{B}(B^\pm \rightarrow \pi^\pm\pi^0) &= (5.12 \pm 0.47 \pm 0.29) \times 10^{-6} \\ \mathcal{B}(B^\pm \rightarrow K^\pm\pi^0) &= (13.3 \pm 0.56 \pm 0.64) \times 10^{-6} \\ C_{\pi^0\pi^0} &= -0.33 \pm 0.36 \pm 0.08 \\ \mathcal{A}_{\pi\pi^0} &= -0.019 \pm 0.088 \pm 0.014 \\ \mathcal{A}_{K\pi^0} &= 0.016 \pm 0.041 \pm 0.012 \end{aligned}$$

The measured values of  $S_{\pi\pi}$  and  $C_{\pi\pi}$  imply that  $CP$  conservation in  $B^0 \rightarrow \pi^+\pi^-$  decays is excluded at the  $3.6\sigma$  level. From these results we present bounds on the CKM angle  $\alpha$ .

Submitted to the 33<sup>rd</sup> International Conference on High-Energy Physics, ICHEP 06,  
26 July—2 August 2006, Moscow, Russia.

---

*Stanford Linear Accelerator Center, Stanford University, Stanford, CA 94309*

---

Work supported in part by Department of Energy contract DE-AC03-76SF00515.

The *BABAR* Collaboration,

B. Aubert, R. Barate, M. Bona, D. Boutigny, F. Couderc, Y. Karyotakis, J. P. Lees, V. Poireau,  
V. Tisserand, A. Zghiche

*Laboratoire de Physique des Particules, IN2P3/CNRS et Université de Savoie, F-74941 Annecy-Le-Vieux,  
France*

E. Grauges

*Universitat de Barcelona, Facultat de Fisica, Departament ECM, E-08028 Barcelona, Spain*

A. Palano

*Università di Bari, Dipartimento di Fisica and INFN, I-70126 Bari, Italy*

J. C. Chen, N. D. Qi, G. Rong, P. Wang, Y. S. Zhu

*Institute of High Energy Physics, Beijing 100039, China*

G. Eigen, I. Ofte, B. Stugu

*University of Bergen, Institute of Physics, N-50007 Bergen, Norway*

G. S. Abrams, M. Battaglia, D. N. Brown, J. Button-Shafer, R. N. Cahn, E. Charles, M. S. Gill,  
Y. Groysman, R. G. Jacobsen, J. A. Kadyk, L. T. Kerth, Yu. G. Kolomensky, G. Kukartsev, G. Lynch,  
L. M. Mir, T. J. Orimoto, M. Pripstein, N. A. Roe, M. T. Ronan, W. A. Wenzel

*Lawrence Berkeley National Laboratory and University of California, Berkeley, California 94720, USA*

P. del Amo Sanchez, M. Barrett, K. E. Ford, A. J. Hart, T. J. Harrison, C. M. Hawkes, S. E. Morgan,  
A. T. Watson

*University of Birmingham, Birmingham, B15 2TT, United Kingdom*

T. Held, H. Koch, B. Lewandowski, M. Pelizaeus, K. Peters, T. Schroeder, M. Steinke  
*Ruhr Universität Bochum, Institut für Experimentalphysik 1, D-44780 Bochum, Germany*

J. T. Boyd, J. P. Burke, W. N. Cottingham, D. Walker

*University of Bristol, Bristol BS8 1TL, United Kingdom*

D. J. Asgeirsson, T. Cuhadar-Donszelmann, B. G. Fulsom, C. Hearty, N. S. Knecht, T. S. Mattison,  
J. A. McKenna

*University of British Columbia, Vancouver, British Columbia, Canada V6T 1Z1*

A. Khan, P. Kyberd, M. Saleem, D. J. Sherwood, L. Teodorescu

*Brunel University, Uxbridge, Middlesex UB8 3PH, United Kingdom*

V. E. Blinov, A. D. Bukin, V. P. Druzhinin, V. B. Golubev, A. P. Onuchin, S. I. Serednyakov,  
Yu. I. Skovpen, E. P. Solodov, K. Yu Todyshev

*Budker Institute of Nuclear Physics, Novosibirsk 630090, Russia*

D. S. Best, M. Bondioli, M. Bruinsma, M. Chao, S. Curry, I. Eschrich, D. Kirkby, A. J. Lankford, P. Lund,  
M. Mandelkern, R. K. Mommesen, W. Roethel, D. P. Stoker

*University of California at Irvine, Irvine, California 92697, USA*

S. Abachi, C. Buchanan

*University of California at Los Angeles, Los Angeles, California 90024, USA*

S. D. Foulkes, J. W. Gary, O. Long, B. C. Shen, K. Wang, L. Zhang  
*University of California at Riverside, Riverside, California 92521, USA*

H. K. Hadavand, E. J. Hill, H. P. Paar, S. Rahatlou, V. Sharma  
*University of California at San Diego, La Jolla, California 92093, USA*

J. W. Berryhill, C. Campagnari, A. Cunha, B. Dahmes, T. M. Hong, D. Kovalskyi, J. D. Richman  
*University of California at Santa Barbara, Santa Barbara, California 93106, USA*

T. W. Beck, A. M. Eisner, C. J. Flacco, C. A. Heusch, J. Kroseberg, W. S. Lockman, G. Nesom, T. Schalk,  
B. A. Schumm, A. Seiden, P. Spradlin, D. C. Williams, M. G. Wilson  
*University of California at Santa Cruz, Institute for Particle Physics, Santa Cruz, California 95064, USA*

J. Albert, E. Chen, A. Dvoretskii, F. Fang, D. G. Hitlin, I. Narsky, T. Piatenko, F. C. Porter, A. Ryd,  
A. Samuel  
*California Institute of Technology, Pasadena, California 91125, USA*

G. Mancinelli, B. T. Meadows, K. Mishra, M. D. Sokoloff  
*University of Cincinnati, Cincinnati, Ohio 45221, USA*

F. Blanc, P. C. Bloom, S. Chen, W. T. Ford, J. F. Hirschauer, A. Kreisel, M. Nagel, U. Nauenberg,  
A. Olivas, W. O. Ruddick, J. G. Smith, K. A. Ulmer, S. R. Wagner, J. Zhang  
*University of Colorado, Boulder, Colorado 80309, USA*

A. Chen, E. A. Eckhart, A. Soffer, W. H. Toki, R. J. Wilson, F. Winklmeier, Q. Zeng  
*Colorado State University, Fort Collins, Colorado 80523, USA*

D. D. Altenburg, E. Feltresi, A. Hauke, H. Jasper, J. Merkel, A. Petzold, B. Spaan  
*Universität Dortmund, Institut für Physik, D-44221 Dortmund, Germany*

T. Brandt, V. Klose, H. M. Lacker, W. F. Mader, R. Nogowski, J. Schubert, K. R. Schubert, R. Schwierz,  
J. E. Sundermann, A. Volk  
*Technische Universität Dresden, Institut für Kern- und Teilchenphysik, D-01062 Dresden, Germany*

D. Bernard, G. R. Bonneau, E. Latour, Ch. Thiebaux, M. Verderi  
*Laboratoire Leprince-Ringuet, CNRS/IN2P3, Ecole Polytechnique, F-91128 Palaiseau, France*

P. J. Clark, W. Gradl, F. Muheim, S. Playfer, A. I. Robertson, Y. Xie  
*University of Edinburgh, Edinburgh EH9 3JZ, United Kingdom*

M. Andreotti, D. Bettoni, C. Bozzi, R. Calabrese, G. Cibinetto, E. Luppi, M. Negrini, A. Petrella,  
L. Piemontese, E. Prencipe  
*Università di Ferrara, Dipartimento di Fisica and INFN, I-44100 Ferrara, Italy*

F. Anulli, R. Baldini-Ferroli, A. Calcaterra, R. de Sangro, G. Finocchiaro, S. Pacetti, P. Patteri,  
I. M. Peruzzi,<sup>1</sup> M. Piccolo, M. Rama, A. Zallo  
*Laboratori Nazionali di Frascati dell'INFN, I-00044 Frascati, Italy*

---

<sup>1</sup>Also with Università di Perugia, Dipartimento di Fisica, Perugia, Italy

A. Buzzo, R. Capra, R. Contri, M. Lo Vetere, M. M. Macri, M. R. Monge, S. Passaggio, C. Patrignani,  
E. Robutti, A. Santroni, S. Tosi

*Università di Genova, Dipartimento di Fisica and INFN, I-16146 Genova, Italy*

G. Brandenburg, K. S. Chaisanguanthum, M. Morii, J. Wu  
*Harvard University, Cambridge, Massachusetts 02138, USA*

R. S. Dubitzky, J. Marks, S. Schenk, U. Uwer

*Universität Heidelberg, Physikalisches Institut, Philosophenweg 12, D-69120 Heidelberg, Germany*

D. J. Bard, W. Bhimji, D. A. Bowerman, P. D. Dauncey, U. Egede, R. L. Flack, J. A. Nash,  
M. B. Nikolich, W. Panduro Vazquez

*Imperial College London, London, SW7 2AZ, United Kingdom*

P. K. Behera, X. Chai, M. J. Charles, U. Mallik, N. T. Meyer, V. Ziegler  
*University of Iowa, Iowa City, Iowa 52242, USA*

J. Cochran, H. B. Crawley, L. Dong, V. Egyes, W. T. Meyer, S. Prell, E. I. Rosenberg, A. E. Rubin  
*Iowa State University, Ames, Iowa 50011-3160, USA*

A. V. Gritsan

*Johns Hopkins University, Baltimore, Maryland 21218, USA*

A. G. Denig, M. Fritsch, G. Schott

*Universität Karlsruhe, Institut für Experimentelle Kernphysik, D-76021 Karlsruhe, Germany*

N. Arnaud, M. Davier, G. Grosdidier, A. Höcker, F. Le Diberder, V. Lepeltier, A. M. Lutz, A. Oyanguren,  
S. Pruvot, S. Rodier, P. Roudeau, M. H. Schune, A. Stocchi, W. F. Wang, G. Wormser

*Laboratoire de l'Accélérateur Linéaire, IN2P3/CNRS et Université Paris-Sud 11, Centre Scientifique  
d'Orsay, B.P. 34, F-91898 ORSAY Cedex, France*

C. H. Cheng, D. J. Lange, D. M. Wright

*Lawrence Livermore National Laboratory, Livermore, California 94550, USA*

C. A. Chavez, I. J. Forster, J. R. Fry, E. Gabathuler, R. Gamet, K. A. George, D. E. Hutchcroft,  
D. J. Payne, K. C. Schofield, C. Touramanis

*University of Liverpool, Liverpool L69 7ZE, United Kingdom*

A. J. Bevan, F. Di Lodovico, W. Menges, R. Sacco

*Queen Mary, University of London, E1 4NS, United Kingdom*

G. Cowan, H. U. Flaecher, D. A. Hopkins, P. S. Jackson, T. R. McMahon, S. Ricciardi, F. Salvatore,  
A. C. Wren

*University of London, Royal Holloway and Bedford New College, Egham, Surrey TW20 0EX, United  
Kingdom*

D. N. Brown, C. L. Davis

*University of Louisville, Louisville, Kentucky 40292, USA*

J. Allison, N. R. Barlow, R. J. Barlow, Y. M. Chia, C. L. Edgar, G. D. Lafferty, M. T. Naisbit,  
J. C. Williams, J. I. Yi

*University of Manchester, Manchester M13 9PL, United Kingdom*

C. Chen, W. D. Hulsbergen, A. Jawahery, C. K. Lae, D. A. Roberts, G. Simi

*University of Maryland, College Park, Maryland 20742, USA*

G. Blaylock, C. Dallapiccola, S. S. Hertzbach, X. Li, T. B. Moore, S. Saremi, H. Staengle

*University of Massachusetts, Amherst, Massachusetts 01003, USA*

R. Cowan, G. Sciolla, S. J. Sekula, M. Spitznagel, F. Taylor, R. K. Yamamoto

*Massachusetts Institute of Technology, Laboratory for Nuclear Science, Cambridge, Massachusetts 02139,  
USA*

H. Kim, S. E. McLachlin, P. M. Patel, S. H. Robertson

*McGill University, Montréal, Québec, Canada H3A 2T8*

A. Lazzaro, V. Lombardo, F. Palombo

*Università di Milano, Dipartimento di Fisica and INFN, I-20133 Milano, Italy*

J. M. Bauer, L. Cremaldi, V. Eschenburg, R. Godang, R. Kroeger, D. A. Sanders, D. J. Summers,  
H. W. Zhao

*University of Mississippi, University, Mississippi 38677, USA*

S. Brunet, D. Côté, M. Simard, P. Taras, F. B. Viaud

*Université de Montréal, Physique des Particules, Montréal, Québec, Canada H3C 3J7*

H. Nicholson

*Mount Holyoke College, South Hadley, Massachusetts 01075, USA*

N. Cavallo,<sup>2</sup> G. De Nardo, F. Fabozzi,<sup>3</sup> C. Gatto, L. Lista, D. Monorchio, P. Paolucci, D. Piccolo,  
C. Sciacca

*Università di Napoli Federico II, Dipartimento di Scienze Fisiche and INFN, I-80126, Napoli, Italy*

M. A. Baak, G. Raven, H. L. Snoek

*NIKHEF, National Institute for Nuclear Physics and High Energy Physics, NL-1009 DB Amsterdam, The  
Netherlands*

C. P. Jessop, J. M. LoSecco

*University of Notre Dame, Notre Dame, Indiana 46556, USA*

T. Allmendinger, G. Benelli, L. A. Corwin, K. K. Gan, K. Honscheid, D. Hufnagel, P. D. Jackson,  
H. Kagan, R. Kass, A. M. Rahimi, J. J. Regensburger, R. Ter-Antonyan, Q. K. Wong

*Ohio State University, Columbus, Ohio 43210, USA*

N. L. Blount, J. Brau, R. Frey, O. Igonkina, J. A. Kolb, M. Lu, R. Rahmat, N. B. Sinev, D. Strom,  
J. Strube, E. Torrence

*University of Oregon, Eugene, Oregon 97403, USA*

<sup>2</sup>Also with Università della Basilicata, Potenza, Italy

<sup>3</sup>Also with Università della Basilicata, Potenza, Italy

A. Gaz, M. Margoni, M. Morandin, A. Pompili, M. Posocco, M. Rotondo, F. Simonetto, R. Stroili, C. Voci  
*Università di Padova, Dipartimento di Fisica and INFN, I-35131 Padova, Italy*

M. Benayoun, H. Briand, J. Chauveau, P. David, L. Del Buono, Ch. de la Vaissière, O. Hamon,  
B. L. Hartfiel, M. J. J. John, Ph. Leruste, J. Malclès, J. Ocariz, L. Roos, G. Therin

*Laboratoire de Physique Nucléaire et de Hautes Energies, IN2P3/CNRS, Université Pierre et Marie Curie-Paris6, Université Denis Diderot-Paris7, F-75252 Paris, France*

L. Gladney, J. Panetta  
*University of Pennsylvania, Philadelphia, Pennsylvania 19104, USA*

M. Biasini, R. Covarelli  
*Università di Perugia, Dipartimento di Fisica and INFN, I-06100 Perugia, Italy*

C. Angelini, G. Batignani, S. Bettarini, F. Bucci, G. Calderini, M. Carpinelli, R. Cenci, F. Forti,  
M. A. Giorgi, A. Lusiani, G. Marchiori, M. A. Mazur, M. Morganti, N. Neri, E. Paoloni, G. Rizzo,  
J. J. Walsh

*Università di Pisa, Dipartimento di Fisica, Scuola Normale Superiore and INFN, I-56127 Pisa, Italy*

M. Haire, D. Judd, D. E. Wagoner  
*Prairie View A&M University, Prairie View, Texas 77446, USA*

J. Biesiada, N. Danielson, P. Elmer, Y. P. Lau, C. Lu, J. Olsen, A. J. S. Smith, A. V. Telnov  
*Princeton University, Princeton, New Jersey 08544, USA*

F. Bellini, G. Cavoto, A. D’Orazio, D. del Re, E. Di Marco, R. Faccini, F. Ferrarotto, F. Ferromi,  
M. Gaspero, L. Li Gioi, M. A. Mazzoni, S. Morganti, G. Piredda, F. Polci, F. Safai Tehrani, C. Voena  
*Università di Roma La Sapienza, Dipartimento di Fisica and INFN, I-00185 Roma, Italy*

M. Ebert, H. Schröder, R. Waldi  
*Universität Rostock, D-18051 Rostock, Germany*

T. Adye, N. De Groot, B. Franek, E. O. Olaiya, F. F. Wilson  
*Rutherford Appleton Laboratory, Chilton, Didcot, Oxon, OX11 0QX, United Kingdom*

R. Aleksan, S. Emery, A. Gaidot, S. F. Ganzhur, G. Hamel de Monchenault, W. Kozanecki, M. Legendre,  
G. Vasseur, Ch. Yèche, M. Zito  
*DSM/Dapnia, CEA/Saclay, F-91191 Gif-sur-Yvette, France*

X. R. Chen, H. Liu, W. Park, M. V. Purohit, J. R. Wilson  
*University of South Carolina, Columbia, South Carolina 29208, USA*

M. T. Allen, D. Aston, R. Bartoldus, P. Bechtle, N. Berger, R. Claus, J. P. Coleman, M. R. Convery,  
M. Cristinziani, J. C. Dingfelder, J. Dorfan, G. P. Dubois-Felsmann, D. Dujmic, W. Dunwoodie,  
R. C. Field, T. Glanzman, S. J. Gowdy, M. T. Graham, P. Grenier,<sup>4</sup> V. Halyo, C. Hast, T. Hrynev’ova,  
W. R. Innes, M. H. Kelsey, P. Kim, D. W. G. S. Leith, S. Li, S. Luitz, V. Luth, H. L. Lynch,  
D. B. MacFarlane, H. Marsiske, R. Messner, D. R. Muller, C. P. O’Grady, V. E. Ozcan, A. Perazzo,  
M. Perl, T. Pulliam, B. N. Ratcliff, A. Roodman, A. A. Salnikov, R. H. Schindler, J. Schwiening,  
A. Snyder, J. Stelzer, D. Su, M. K. Sullivan, K. Suzuki, S. K. Swain, J. M. Thompson, J. Va’vra, N. van

---

<sup>4</sup>Also at Laboratoire de Physique Corpusculaire, Clermont-Ferrand, France

Bakel, M. Weaver, A. J. R. Weinstein, W. J. Wisniewski, M. Wittgen, D. H. Wright, A. K. Yarritu, K. Yi,  
C. C. Young

*Stanford Linear Accelerator Center, Stanford, California 94309, USA*

P. R. Burchat, A. J. Edwards, S. A. Majewski, B. A. Petersen, C. Roat, L. Wilden  
*Stanford University, Stanford, California 94305-4060, USA*

S. Ahmed, M. S. Alam, R. Bula, J. A. Ernst, V. Jain, B. Pan, M. A. Saeed, F. R. Wappler, S. B. Zain  
*State University of New York, Albany, New York 12222, USA*

W. Bugg, M. Krishnamurthy, S. M. Spanier  
*University of Tennessee, Knoxville, Tennessee 37996, USA*

R. Eckmann, J. L. Ritchie, A. Satpathy, C. J. Schilling, R. F. Schwitters  
*University of Texas at Austin, Austin, Texas 78712, USA*

J. M. Izen, X. C. Lou, S. Ye  
*University of Texas at Dallas, Richardson, Texas 75083, USA*

F. Bianchi, F. Gallo, D. Gamba

*Università di Torino, Dipartimento di Fisica Sperimentale and INFN, I-10125 Torino, Italy*

M. Bomben, L. Bosisio, C. Cartaro, F. Cossutti, G. Della Ricca, S. Dittongo, L. Lanceri, L. Vitale  
*Università di Trieste, Dipartimento di Fisica and INFN, I-34127 Trieste, Italy*

V. Azzolini, N. Lopez-March, F. Martinez-Vidal  
*IFIC, Universitat de Valencia-CSIC, E-46071 Valencia, Spain*

Sw. Banerjee, B. Bhuyan, C. M. Brown, D. Fortin, K. Hamano, R. Kowalewski, I. M. Nugent, J. M. Roney,  
R. J. Sobie

*University of Victoria, Victoria, British Columbia, Canada V8W 3P6*

J. J. Back, P. F. Harrison, T. E. Latham, G. B. Mohanty, M. Pappagallo  
*Department of Physics, University of Warwick, Coventry CV4 7AL, United Kingdom*

H. R. Band, X. Chen, B. Cheng, S. Dasu, M. Datta, K. T. Flood, J. J. Hollar, P. E. Kutter, B. Mellado,  
A. Mihalyi, Y. Pan, M. Pierini, R. Prepost, S. L. Wu, Z. Yu  
*University of Wisconsin, Madison, Wisconsin 53706, USA*

H. Neal

*Yale University, New Haven, Connecticut 06511, USA*

# 1 INTRODUCTION

$CP$ -violating processes are incisive tests of the Cabibbo-Kabayashi-Maskawa (CKM) model of quark mixing [1]. Measurements with small theoretical uncertainties in the CKM model provide the most effective constraints on physics outside this model. The CKM Unitarity Triangle angle  $\alpha \equiv \arg [-V_{\text{td}} V_{\text{tb}}^*/V_{\text{ud}} V_{\text{ub}}^*]$  is measured through the interference of  $b \rightarrow u$  quark-level decays and  $B^0 \leftrightarrow \bar{B}^0$  mixing. Multiple measurements of  $\alpha$ , with different decays, further test the consistency of the CKM model. The time-dependent asymmetry in  $B^0 \rightarrow \pi^+ \pi^-$  is proportional to  $\sin 2\alpha$  in the limit that only one amplitude contributes to this decay. However, measurements of an unexpectedly large branching fraction for  $B^0 \rightarrow \pi^0 \pi^0$  compared to that of  $B^\pm \rightarrow \pi^\pm \pi^0$  and  $B^0 \rightarrow \pi^+ \pi^-$  [2] indicate that both  $b \rightarrow u$  (tree) and  $b \rightarrow d$  (penguin) amplitudes, with different weak phases, are present. Thus, the time-dependent asymmetry is modified to

$$\begin{aligned} a(\Delta t) &= \frac{|\bar{A}(\Delta t)|^2 - |A(\Delta t)|^2}{|\bar{A}(\Delta t)|^2 + |A(\Delta t)|^2} = S_{\pi\pi} \sin(\Delta m_d \Delta t) - C_{\pi\pi} \cos(\Delta m_d \Delta t) \\ C_{\pi\pi} &= \frac{|A|^2 - |\bar{A}|^2}{|A|^2 + |\bar{A}|^2} \\ S_{\pi\pi} &= \sqrt{1 - C_{\pi\pi}^2} \sin(2\alpha - 2\Delta\alpha_{\pi\pi}), \end{aligned} \quad (1)$$

where  $\Delta t$  is the difference between the proper decay times and  $\Delta m_d$  is the  $B$ -meson mixing frequency. Both the total phase difference  $\Delta\alpha_{\pi\pi}$  and  $C_{\pi\pi}$  may differ from zero due to a penguin contribution to the decay amplitude  $A$ .

The magnitude and relative phase of the penguin contribution to the asymmetry may be unraveled with an isospin relation between the three  $B \rightarrow \pi\pi$  decays [3]. The amplitudes  $A^{ij}$  for the  $B \rightarrow \pi^i \pi^j$  decays satisfy the relation

$$A^{+0} = \frac{1}{\sqrt{2}} A^{+-} + A^{00}, \quad (2)$$

with a similar expression for the conjugate amplitudes. The shape of the corresponding isospin triangle is determined from measurements of the branching fraction and time-integrated  $CP$  asymmetry for each  $B \rightarrow \pi\pi$  decay. We define the direct  $CP$  asymmetry as

$$\begin{aligned} C_{\pi^0 \pi^0} &= \frac{|A^{00}|^2 - |\bar{A}^{00}|^2}{|A^{00}|^2 + |\bar{A}^{00}|^2} \\ \mathcal{A}_{\pi\pi^0} &= \frac{|\bar{A}^{-0}|^2 - |A^{+0}|^2}{|\bar{A}^{-0}|^2 + |A^{+0}|^2}. \end{aligned} \quad (3)$$

From the difference in shape of these triangles for  $B^0$  and  $\bar{B}^0$ ,  $\Delta\alpha_{\pi\pi}$  may be determined up to a four-fold ambiguity. No  $CP$  asymmetry is expected in the  $\Delta I = 3/2$  decay  $B^\pm \rightarrow \pi^\pm \pi^0$ , where no penguin amplitudes are present.

The phenomenology of the  $B \rightarrow \pi\pi$  system has been studied in a variety of theoretical frameworks and models [4]. Predictions for the relative size and phase of the penguin contribution vary considerably, so more precise measurements will help to distinguish among different theoretical approaches and add to our understanding of hadronic  $B$  decays.

In addition to the unexpected pattern of decay rates in the  $B \rightarrow \pi\pi$  system mentioned above, the measured rates and direct  $CP$ -violating asymmetries in  $B \rightarrow K\pi$  decays [5, 6, 7] reveal puzzling features that could indicate significant contributions from electroweak (EW) penguins [8, 9].

Various methods have been proposed to isolate the Standard Model contribution to this process in order to test for signs of new physics. Sum rules derived from  $U$ -spin symmetry relate the rates and asymmetries for the decays  $B^0$  or  $B^+$  to  $K^+\pi^-$ ,  $K^+\pi^0$ ,  $K^0\pi^0$ , and  $K^0\pi^+$  [10], while  $SU(3)$  symmetry can be used to make predictions for the  $K\pi$  system based on hadronic parameters extracted from the  $\pi\pi$  system [8].

## 2 THE *BABAR* DETECTOR AND DATASET

The data used in this analysis were collected in 1999–2006 with the *BABAR* detector at the PEP-II asymmetric-energy  $B$ -meson factory at the Stanford Linear Accelerator Center. A total of 347 million  $B\bar{B}$  pairs were used. The preliminary results presented here supersede the results in three prior publications [11]. Roughly 120 million more  $B\bar{B}$  decays have been added, and a number of improvements have been introduced to the data analysis, effectively increasing the acceptance for the modes containing a neutral pion.

The *BABAR* detector is described in detail elsewhere [12]. Charged-particle (track) momenta are measured with a 5-layer double-sided silicon vertex tracker (SVT) and a 40-layer drift chamber (DCH) inside a 1.5-T superconducting solenoidal magnet. Neutral-cluster (photon) positions and energies are measured with an electromagnetic calorimeter (EMC) consisting of 6580 CsI(Tl) crystals. The photon energy resolution is  $\sigma_E/E = \{2.3/E(\text{GeV})^{1/4} \oplus 1.9\}\%$ , and the angular resolution from the interaction point is  $\sigma_\theta = 3.9^\circ/\sqrt{E(\text{GeV})}$ . Charged hadrons are identified with a detector of internally reflected Cherenkov light (DIRC) and ionization measurements in the tracking detectors. The average  $K$ – $\pi$  separation in the DIRC varies from  $12\sigma$  at a laboratory momentum of 1.5 GeV/ $c$  to  $2\sigma$  at 4.5 GeV/ $c$ .

## 3 ANALYSIS METHOD

Many elements of the  $B \rightarrow \pi\pi$  measurements are common to the three groups of decay modes  $B^0 \rightarrow h^+h'^-$  ( $h = \pi$  or  $K$ ),  $B^0 \rightarrow \pi^0\pi^0$ , and  $B^\pm \rightarrow h^\pm\pi^0$ .  $B$  candidates ( $B_{\text{rec}}$ ) are formed by combining two particles, either tracks or  $\pi^0$  candidates.

### 3.1 Track and Cluster Selection

For the  $B^\pm \rightarrow h^\pm\pi^0$  and the  $B^0 \rightarrow h^+h'^-$  samples, we require that each track have an associated Cherenkov angle ( $\theta_C$ ) measured with more than five signal photons detected in the DIRC, where the value of  $\theta_C$  must agree with either the pion or kaon particle hypothesis to within  $4\sigma$ . The last requirement efficiently removes events containing high-momentum protons. Electrons are removed based on energy-loss measurements in the SVT and DCH, and on a comparison of the track momentum and the associated energy deposited in the EMC.

The  $\pi^0$  candidates are formed from two EMC clusters, one EMC cluster containing two nearby photons (merged  $\pi^0$ ), or one EMC cluster and two tracks from a photon conversion to an  $e^+e^-$  pair inside the detector. Previous *BABAR* results for  $B^0 \rightarrow \pi^0\pi^0$  and  $B^\pm \rightarrow h^\pm\pi^0$  only included  $\pi^0$  from two EMC clusters; the addition of merged  $\pi^0$  and converted photons increases the  $\pi^0$  efficiency by 10%. Clusters are required to have a transverse energy deposit consistent with a photon, and to have an energy  $E_\gamma > 0.03$  GeV. To reduce the background from random photon combinations, the angle  $\theta_\gamma$  between the photon momentum vector in the  $\pi^0$  rest frame and the  $\pi^0$  momentum

vector in the laboratory frame is required to satisfy  $|\cos \theta_\gamma| < 0.95$ . The  $\pi^0$  candidates are fitted kinematically with their mass constrained to the nominal  $\pi^0$  mass.

Photon conversions are selected from pairs of oppositely charged tracks with invariant mass less than 30 MeV/ $c^2$  and whose momentum vector points to the beamspot. The conversion point is required to lie inside the detector material. Photons from conversions are combined with photons from single EMC clusters to form  $\pi^0$  candidates.

Single EMC clusters containing two photons are selected with the transverse second moment,  $S = \sum_i E_i \times (\Delta\alpha_i)^2 / E$ , where  $E_i$  is energy in each CsI(Tl) crystal and  $\Delta\alpha_i$  is the angle between the cluster centroid and the crystal. The second moment is used to distinguish merged  $\pi^0$  candidates from both single photons and neutral hadrons.

### 3.2 Event Selection

Two kinematic variables are used to separate  $B$  decays from the large  $e^+e^- \rightarrow q\bar{q}$  ( $q = u, d, s, c$ ) background: the beam-energy-substituted mass  $m_{\text{ES}} = \sqrt{(s/2 + \mathbf{p}_i \cdot \mathbf{p}_B)^2 / E_i^2 - \mathbf{p}_B^2}$ , where  $\sqrt{s}$  is the total  $e^+e^-$  center-of-mass (CM) energy,  $(E_i, \mathbf{p}_i)$  is the four-momentum of the initial  $e^+e^-$  system and  $\mathbf{p}_B$  is the  $B$ -candidate momentum, both measured in the laboratory frame, and  $\Delta E = E_B - \sqrt{s}/2$ , where  $E_B$  is the  $B$ -candidate energy in the CM frame.

Two additional quantities take advantage of the event topology to further separate  $B$  decays from  $q\bar{q}$  background. The cosine of the angle  $\theta_S$  between the sphericity axes of the  $B$  candidate's decay products and that of the remaining tracks and clusters in the event, in the CM frame, is peaked at  $\pm 1.0$  for jet-like  $q\bar{q}$  events, but has a flat distribution for  $B$  decays. We require  $|\cos \theta_S| < 0.7$  (0.8) for  $B^0 \rightarrow \pi^0\pi^0$  ( $B^\pm \rightarrow h^\pm\pi^0$  and  $B^0 \rightarrow h^+h'^-$ ). For just the  $B^0 \rightarrow h^+h'^-$  sample, we further require that the second Fox-Wolfram moment satisfy  $R_2 < 0.7$  to remove a small remaining background from  $\tau$ -pair events. To improve the discrimination against  $q\bar{q}$  events, a Fisher discriminant  $\mathcal{F}$  is formed from the sums  $\sum_i p_i$  and  $\sum_i p_i \cos^2 \theta_i$ , where  $p_i$  is the momentum and  $\theta_i$  is the angle with respect to the thrust axis of the  $B$  candidate, both in the CM frame, of all tracks and clusters not used to reconstruct the  $B$  meson.

The number of  $B$  decays and the corresponding  $CP$  asymmetries are determined in extended unbinned maximum likelihood (ML) fits to the variables  $m_{\text{ES}}$ ,  $\Delta E$ , and  $\mathcal{F}$ , plus additional information as described below. The likelihood is given by the expression

$$\mathcal{L} = \exp \left( - \sum_i^M n_i \right) \prod_j^N \left[ \sum_i^M n_i \mathcal{P}_i(\vec{x}_j; \vec{\alpha}_i) \right], \quad (4)$$

where the product is over the number of events  $N$ , the sums are over the event categories  $M$ ,  $n_i$  is the coefficient for each category as described below, and the probability density function (PDF)  $\mathcal{P}$  describes the distribution of the variables  $\vec{x}$  in terms of parameters  $\vec{\alpha}$ .

### 3.3 $B^0 \rightarrow \pi^+\pi^-$ and $B^0 \rightarrow K^+\pi^-$

The time-dependent  $CP$  asymmetry measurement in  $B^0 \rightarrow \pi^+\pi^-$  also uses  $B$ -flavor, decay-time, and particle-identification information to separate  $B^0 \rightarrow \pi^+\pi^-$  and  $B^0 \rightarrow K^+\pi^-$  decays and measure their  $CP$  asymmetries.

The variables  $m_{\text{ES}}$  and  $\Delta E$  are calculated assuming that both tracks are charged pions.  $B \rightarrow \pi\pi$  events are described by a Gaussian distribution for both  $m_{\text{ES}}$  and  $\Delta E$ , with resolutions of 2.5 MeV/ $c^2$  and 28 MeV, respectively. For each kaon in the final state, the  $\Delta E$  peak position is shifted from

zero by an amount that depends on the kaon momentum, with an average shift of  $-45$  MeV. We require  $5.20 < m_{\text{ES}} < 5.29 \text{ GeV}/c^2$  and  $|\Delta E| < 0.150 \text{ GeV}$ . The large region below the signal in  $m_{\text{ES}}$  effectively determines the background shape parameters, while the wide range in  $\Delta E$  allows us to separate  $B$  decays to all four final states in the same fit.

The Cherenkov angle  $\theta_C$  measured by the DIRC is used to further separate charged kaons and pions. The difference between the measured and expected values of  $\theta_C$ , divided by its uncertainty, is modeled by a sum of two Gaussian distributions. The  $\theta_C$  PDF is parametrized separately for  $K^+$ ,  $K^-$ ,  $\pi^+$ , and  $\pi^-$  tracks as a function of momentum and polar angle.

We use a multivariate technique [13] to determine the flavor of the other  $B$  meson ( $B_{\text{tag}}$ ). Separate neural networks are trained to identify primary leptons, kaons, soft pions from  $D^*$  decays, and high-momentum charged particles from  $B$  decays. Events are assigned to one of seven mutually exclusive tagging categories (including untagged events) based on the estimated average mistag probability and the source of the tagging information (Table 1). The quality of tagging is expressed in terms of the effective efficiency  $Q = \sum_k \epsilon_k(1 - 2w_k)^2$ , where  $\epsilon_k$  and  $w_k$  are the efficiencies and mistag probabilities, respectively, for events tagged in category  $k$ . The difference in mistag probabilities is given by  $\Delta w = w_{B^0} - w_{\bar{B}^0}$ . Table 1 summarizes the tagging performance measured in a data sample of fully reconstructed neutral  $B$  decays to  $D^{(*)-}(\pi^+, \rho^+, a_1^+)$  ( $B_{\text{flav}}$ ).

The time difference  $\Delta t = \Delta z/\beta\gamma c$  is obtained from the known boost of the  $e^+e^-$  system ( $\beta\gamma = 0.56$ ) and the measured distance  $\Delta z$  along the beam ( $z$ ) axis between the  $B_{\text{rec}}$  and  $B_{\text{tag}}$  decay vertices. We require  $|\Delta t| < 20 \text{ ps}$  and  $\sigma_{\Delta t} < 2.5 \text{ ps}$ , where  $\sigma_{\Delta t}$  is the error on  $\Delta t$  determined separately for each event. The signal  $\Delta t$  PDF for  $B^0 \rightarrow \pi^+\pi^-$  is given by

$$f_k^\pm(\Delta t_{\text{meas}}) = \frac{e^{-|\Delta t|/\tau}}{4\tau} \left\{ (1 \mp \Delta w) \right. \\ \left. \pm (1 - 2w_k)[S_{\pi\pi} \sin(\Delta m_d \Delta t) - C_{\pi\pi} \cos(\Delta m_d \Delta t)] \right\} \otimes R(\Delta t_{\text{meas}} - \Delta t), \quad (5)$$

where  $f_k^+$  ( $f_k^-$ ) indicates a  $B^0$  ( $\bar{B}^0$ ) flavor tag, and where index  $k$  is the tagging category. The resolution function  $R(\Delta t_{\text{meas}} - \Delta t)$  for signal candidates is a sum of three Gaussians, identical to the one described in Ref. [13], with parameters determined from a fit to the  $B_{\text{flav}}$  sample (including events in all seven tagging categories). The background  $\Delta t$  distribution is modeled as the sum of three Gaussian functions, where the common parameters used to describe the background shape for all tagging categories are determined simultaneously with the  $CP$  parameters in the maximum likelihood fit.

The ML fit includes eight components:  $B$  decays and background with the final states  $\pi^+\pi^-$ ,  $K^+\pi^-$ ,  $K^-\pi^+$ , and  $K^+K^-$ . The component coefficients for  $K\pi$  are parametrized as  $n_{K^\pm\pi^\mp} = n_{K\pi}(1 \mp \mathcal{A}_{K\pi})/2$ , where  $\mathcal{A}_{K\pi}$  is the direct  $CP$ -violating asymmetry. All other coefficients are the product of the fraction of events in each tagging category, taken from  $B_{\text{flav}}$  events, and the event yield. The background PDFs are a threshold function for  $m_{\text{ES}}$  and a polynomial for  $\Delta E$ . The  $\mathcal{F}$  PDF is a double Gaussian for the background and an asymmetric Gaussian for the signal. All background PDF parameters are allowed to float in the ML fit.

### 3.4 $B^0 \rightarrow \pi^0\pi^0$

$B^0 \rightarrow \pi^0\pi^0$  events are identified with an ML fit to the variables  $m_{\text{ES}}$ ,  $\Delta E$ , and  $\mathcal{F}$ . For  $B^0 \rightarrow \pi^0\pi^0$ , we require  $m_{\text{ES}} > 5.20 \text{ GeV}/c^2$  and  $|\Delta E| < 0.2 \text{ GeV}$ . Tails in the EMC response produce a correlation between  $m_{\text{ES}}$  and  $\Delta E$ , so a two-dimensional PDF, derived from Monte Carlo (MC)

simulation, is used. The PDF for  $\mathcal{F}$  is a step function, with parameters taken from MC.  $B_{\text{flav}}$  data is used to verify that the MC accurately reproduces the  $\mathcal{F}$  distribution. The  $q\bar{q}$  background PDFs are a threshold function for  $m_{\text{ES}}$ , a polynomial for  $\Delta E$ , and a step function for  $\mathcal{F}$ . All  $q\bar{q}$  background PDF parameters are allowed to float in the ML fit.

The decays  $B^+ \rightarrow \rho^+\pi^0$  and  $B^0 \rightarrow K^0\pi^0 (K_S^0 \rightarrow \pi^0\pi^0)$  add  $52 \pm 6.8$  background events to  $B^0 \rightarrow \pi^0\pi^0$  and are included as an additional fixed component in the ML fit. We model these  $B$  backgrounds with a two-dimensional PDF to describe  $m_{\text{ES}}$  and  $\Delta E$  and with a step function for  $\mathcal{F}$ , all taken from MC simulation.

The time-integrated  $CP$  asymmetry is measured by the  $B$ -flavor tagging described previously. The fraction of events in each tagging category is also constrained to the fractions determined from MC simulation. The PDF coefficient for the  $B^0 \rightarrow \pi^0\pi^0$  signal is given by the expression

$$n_{\pi^0\pi^0,k} = \frac{1}{2} f_k N_{\pi^0\pi^0} \left\{ 1 - s_j(1 - 2\chi)(1 - 2w_k) C_{\pi^0\pi^0} \right\}, \quad (6)$$

where  $f_k$  is the fraction of events in tagging category  $k$ ,  $N_{\pi^0\pi^0}$  is the number of  $B$  decays,  $\chi = 0.184 \pm 0.004$  [14] is the time-integrated mixing probability, and  $s_j = +1(-1)$  when the  $B_{\text{tag}}$  is a  $B^0$  ( $\bar{B}^0$ ).

### 3.5 $B^\pm \rightarrow \pi^\pm\pi^0$ and $B^\pm \rightarrow K^\pm\pi^0$

$B^\pm \rightarrow \pi^\pm\pi^0$  and  $B^\pm \rightarrow K^\pm\pi^0$  events are identified in an ML fit to the variables  $m_{\text{ES}}$ ,  $\Delta E$ ,  $\mathcal{F}$ , and  $\theta_C$ . We require  $B$  candidates to satisfy  $m_{\text{ES}} > 5.22 \text{ GeV}/c^2$  and  $-0.11 < \Delta E < 0.15 \text{ GeV}$ . The tighter requirement on  $\Delta E$  serves to remove  $B$ -decay backgrounds. The treatment of  $\Delta E$  and the use of the Cherenkov angle for kaons and pions is identical to that in  $B^0 \rightarrow \pi^+\pi^-$ . The  $\mathcal{F}$  distribution is also described with a step function, with parameters taken from MC simulation. The  $q\bar{q}$  background PDFs are a threshold function for  $m_{\text{ES}}$ , a polynomial for  $\Delta E$ , and a step function for  $\mathcal{F}$ . All  $q\bar{q}$  background PDF parameters are floating in the ML fit.

Several charmless  $B$  decays with both a high momentum charged track and a  $\pi^0$  or photon appear as background; significant contributions, as determined with MC, come from the following decay modes with the estimated number of events provided in parentheses:  $B^0 \rightarrow \rho^+\pi^-$  ( $32 \pm 3$  events),  $B^+ \rightarrow \rho^+\pi^0$  ( $20 \pm 2$ ),  $B \rightarrow X_s\gamma$  ( $5.8 \pm 0.6$ ),  $B^\pm \rightarrow K^0\pi^\pm (K_S^0 \rightarrow \pi^0\pi^0)$  ( $5.0 \pm 0.3$ ), and  $B^0 \rightarrow \rho^+K^-$  ( $3.3 \pm 0.5$ ). These events, as well as their measured  $CP$  asymmetry, are included as an additional fixed component in the ML fit.

The PDF coefficient for  $B^\pm \rightarrow \pi^\pm\pi^0$  and  $B^\pm \rightarrow K^\pm\pi^0$  signal is given by the expression

$$n_i = \frac{1}{2} N_i (1 - q_j \mathcal{A}_i), \quad (7)$$

where  $\mathcal{A}_i$  is the direct  $CP$  asymmetry and  $q_j$  is the charge of the  $B$  candidate.

## 4 RESULTS AND SYSTEMATIC UNCERTAINTIES

Results from the ML fits for the  $B^0 \rightarrow \pi^0\pi^0$  and  $B^\pm \rightarrow h^\pm\pi^0$  decay modes are summarized in Table 2. Distributions of  $m_{\text{ES}}$ ,  $\Delta E$ , and  $\mathcal{F}$  for  $B^0 \rightarrow \pi^0\pi^0$  are in Fig. 1, where a signal-enhanced subset of the data is shown. The  $B^\pm \rightarrow h^\pm\pi^0$  data are shown in Fig. 2. With a large signal in both decay modes, we show weighted and background-subtracted plots [15] for the  $B^\pm \rightarrow \pi^\pm\pi^0$  and  $B^\pm \rightarrow K^\pm\pi^0$  signal. The same technique is used to display the  $q\bar{q}$  background as well.

The uncertainty in the efficiency for the  $B^0 \rightarrow \pi^0\pi^0$  decay mode is dominated by a 3% systematic uncertainty per  $\pi^0$ , estimated from a study of  $\tau \rightarrow \pi\pi^0\nu_\tau$  decays. There is an additional 3.6% uncertainty from our knowledge of the EMC resolution function, based on a study of the resolution of the  $\pi^0$  mass and the energy of the photon in  $e^+e^- \rightarrow \mu^+\mu^-\gamma$  events. Systematic uncertainties involving the ML fit are evaluated by varying the PDF parameters and refitting the data. The changes in the  $m_{\text{ES}}$  and  $\Delta E$  signal PDFs are taken from the difference in these quantities in the  $B^\pm \rightarrow h^\pm\pi^0$  sample between data and MC. The change in the result is taken as the systematic error. All sources of systematic error for  $B^0 \rightarrow \pi^0\pi^0$  are listed in Table 3.

The largest uncertainties in the  $B^\pm \rightarrow h^\pm\pi^0$  decays arise from uncertainty in the  $m_{\text{ES}}$  and  $\Delta E$  PDFs, our knowledge of the signal  $\mathcal{F}$  distribution evaluated from a sample of  $B^\pm$  decays, and the 3%  $\pi^0$  efficiency uncertainty. The size of a small bias in the ML fit is included as a systematic error. The dominant uncertainty on the direct  $CP$  asymmetries are taken from the size and error in the asymmetry fit in the  $q\bar{q}$  background and the effect of  $CP$  violation in the  $B$  backgrounds. The uncertainties in  $B^\pm \rightarrow h^\pm\pi^0$  are summarized in Table 4.

All results for the  $B^0 \rightarrow h^+h'^-$  decay modes are listed in Table 5. The correlation coefficient between  $S_{\pi\pi}$  and  $C_{\pi\pi}$  is found to be  $-0.082$ . The data distributions of  $m_{\text{ES}}$ ,  $\Delta E$ , and  $\mathcal{F}$  for  $B^0 \rightarrow h^+h'^-$  decays are shown in Fig. 3 for signal and Fig. 4 for background with the event-weighting technique. The direct  $CP$  asymmetry in  $B^0 \rightarrow K^+\pi^-$  is apparent in the distribution of  $\Delta E$  for  $B^0$  and  $\bar{B}^0$  decays, shown in Fig. 5. We show the distributions of  $\Delta t$  for signal and background decays in Fig. 6. In Fig. 7, we show the distribution of  $\Delta t$  separately for  $B^0 \rightarrow \pi^+\pi^-$  events tagged as  $B^0$  or  $\bar{B}^0$ , and the asymmetry  $a(\Delta t)$ . The central values and errors for  $S_{\pi\pi}$  and  $C_{\pi\pi}$  are shown in Fig. 8, along with confidence-level contours. Our measurement excludes the absence of  $CP$  violation ( $S_{\pi\pi} = 0, C_{\pi\pi} = 0$ ) at a confidence level of 0.99970, or  $3.6\sigma$ .

Systematic uncertainties for the  $CP$  asymmetries  $\mathcal{A}_{K\pi}$ ,  $S_{\pi\pi}$ , and  $C_{\pi\pi}$  are listed in Table 6. For the asymmetry in the  $K^+\pi^-$  mode, we find a background asymmetry of  $-0.0042 \pm 0.0064$ , which is consistent with zero. We therefore take the sum in quadrature of the central value of the background asymmetry and its statistical uncertainty as the systematic uncertainty on the signal  $\mathcal{A}_{K\pi}$  to account for possible charge-dependent detector and analysis bias. To further check for biases in the fitting technique, we perform a large number of pseudo-experiments where the signal events are randomly sampled from simulated MC events, and the background is generated directly from the PDFs. We find a bias in  $\mathcal{A}_{K\pi}$  of 0.002 and include this in the systematic uncertainty. The biases on  $S_{\pi\pi}$  and  $C_{\pi\pi}$  in this study are consistent with zero, so we take the sum in quadrature of the central value and its uncertainty as the systematic error due to potential bias in the fitter. The remaining systematic effects for  $S_{\pi\pi}$  and  $C_{\pi\pi}$  are dominated by uncertainties in the parameterization of  $B$ -flavor tagging and vertexing, and (for  $C_{\pi\pi}$ ) in the effect of  $CP$  violation on the tag side.

## 5 CONCLUSIONS

The branching-fraction and  $CP$ -asymmetry results described in this paper are:

$$\begin{aligned}
S_{\pi\pi} &= -0.53 \pm 0.14 \pm 0.02 \\
C_{\pi\pi} &= -0.16 \pm 0.11 \pm 0.03 \\
A_{K\pi} &= -0.108 \pm 0.024 \pm 0.008 \\
\mathcal{B}(B^0 \rightarrow \pi^0 \pi^0) &= (1.48 \pm 0.26 \pm 0.12) \times 10^{-6} \\
\mathcal{B}(B^\pm \rightarrow \pi^\pm \pi^0) &= (5.12 \pm 0.47 \pm 0.29) \times 10^{-6} \\
\mathcal{B}(B^\pm \rightarrow K^\pm \pi^0) &= (13.3 \pm 0.56 \pm 0.64) \times 10^{-6} \\
C_{\pi^0 \pi^0} &= -0.33 \pm 0.36 \pm 0.08 \\
A_{\pi\pi^0} &= -0.019 \pm 0.088 \pm 0.014 \\
A_{K\pi^0} &= 0.016 \pm 0.041 \pm 0.012.
\end{aligned}$$

Combining these with a branching fraction  $\mathcal{B}(B^0 \rightarrow \pi^+ \pi^-) = (5.8 \pm 0.4 \pm 0.3) \times 10^{-6}$ , also measured by *BABAR* [16], we may evaluate the constraints on both the penguin contribution to  $\alpha$  and on the CKM angle  $\alpha$  itself. Constraints are evaluated by scanning the parameters of interest,  $|\Delta\alpha_{\pi\pi}| = |\alpha - \alpha_{\text{eff}}|$  and  $\alpha$ , and then calculating the  $\chi^2$  for the five amplitudes ( $A^{+0}$ ,  $A^{+-}$ ,  $A^{00}$ ,  $\tilde{A}^{+-}$ ,  $\tilde{A}^{00}$ ) given our measurements and the isospin-triangle relations [17]. The  $\chi^2$  is converted to a confidence level (C.L.) as shown in Fig. 9. The upper bound on  $|\Delta\alpha_{\pi\pi}|$  is  $41^\circ$  at the 90% C.L. Somewhat more restrictive new constraints on  $\alpha$  are found from measurements of  $B \rightarrow \rho\rho$  and  $B \rightarrow \rho\pi$  decays [18].

We have also presented updated preliminary measurements of the branching fraction for  $K^+ \pi^0$ , and the charge asymmetries in  $K^+ \pi^-$  and  $K^+ \pi^0$ . Ignoring color-suppressed tree amplitudes, the charge asymmetries in  $K^+ \pi^-$  and  $K^+ \pi^0$  should be equal (see Gronau and Rosner in Ref. [10]), which has not been supported by recent data [5]. The values of  $A_{K\pi}$  and  $A_{K\pi^0}$  reported here are separated by over two standard deviations. These results could indicate a large color-suppressed amplitude, an enhanced electroweak penguin, or possibly new-physics effects [19].

## 6 ACKNOWLEDGMENTS

We are grateful for the extraordinary contributions of our PEP-II colleagues in achieving the excellent luminosity and machine conditions that have made this work possible. The success of this project also relies critically on the expertise and dedication of the computing organizations that support *BABAR*. The collaborating institutions wish to thank SLAC for its support and the kind hospitality extended to them. This work is supported by the US Department of Energy and National Science Foundation, the Natural Sciences and Engineering Research Council (Canada), Institute of High Energy Physics (China), the Commissariat à l'Energie Atomique and Institut National de Physique Nucléaire et de Physique des Particules (France), the Bundesministerium für Bildung und Forschung and Deutsche Forschungsgemeinschaft (Germany), the Istituto Nazionale di Fisica Nucleare (Italy), the Foundation for Fundamental Research on Matter (The Netherlands), the Research Council of Norway, the Ministry of Science and Technology of the Russian Federation, Ministerio de Educación y Ciencia (Spain), and the Particle Physics and Astronomy Research Council (United Kingdom). Individuals have received support from the Marie-Curie IEF program (European Union) and the A. P. Sloan Foundation.

## References

- [1] N. Cabibbo, Phys. Rev. Lett. **10**, 531 (1963); M. Kobayashi and T. Maskawa, Prog. Theor. Phys. **49**, 652 (1973).
- [2] B. Aubert *et al.* [BABAR Collaboration], Phys. Rev. Lett. **94**, 181802 (2005), K. Abe *et al.* [Belle Collaboration], Phys. Rev. Lett. **94**, 181803 (2005).
- [3] M. Gronau and D. London, Phys. Rev. Lett. **65**, 3381 (1990).
- [4] M. Beneke and M. Neubert, Nucl. Phys. B **675**, 333 (2003); C. W. Bauer, D. Pirjol, I. Z. Rothstein and I. W. Stewart, Phys. Rev. D **70**, 054015 (2004); Y. Y. Keum, H. n. Li and A. I. Sanda, AIP Conf. Proc. **618**, 229 (2002); M. Ciuchini, E. Franco, G. Martinelli, M. Pierini and L. Silvestrini, Phys. Lett. B **515**, 33 (2001).
- [5] B. Aubert *et al.* [BABAR Collaboration], hep-ex/0608003, submitted to Phys. Rev. D; B. Aubert *et al.* [BABAR Collaboration], Phys. Rev. Lett. **95**, 221801 (2005); B. Aubert *et al.* [BABAR Collaboration], Phys. Rev. D **71**, 111102 (2005); B. Aubert *et al.* [BABAR Collaboration], Phys. Rev. Lett. **94**, 181802 (2005).
- [6] K. Abe *et al.* [Belle Collaboration], Phys. Rev. Lett. **95**, 231802 (2005); Y. Chao *et al.* [Belle Collaboration], Phys. Rev. D **71**, 031502 (2005); Y. Chao *et al.* [Belle Collaboration], Phys. Rev. D **69**, 111102 (2004).
- [7] A. Bornheim *et al.* [CLEO Collaboration], Phys. Rev. D **68**, 052002 (2003).
- [8] A. J. Buras and R. Fleischer, Eur. Phys. J. C **16**, 97 (2000); A. J. Buras, R. Fleischer, S. Recksiegel and F. Schwab, Phys. Rev. Lett. **92**, 101804 (2004); A. J. Buras, R. Fleischer, S. Recksiegel and F. Schwab, Nucl. Phys. B **697**, 133 (2004).
- [9] M. Gronau and J. L. Rosner, Phys. Lett. B **572**, 43 (2003); T. Yoshikawa, Phys. Rev. D **68**, 054023 (2003); V. Barger, C. W. Chiang, P. Langacker and H. S. Lee, Phys. Lett. B **598**, 218 (2004); S. Mishima and T. Yoshikawa, Phys. Rev. D **70**, 094024 (2004); Y.-L. Wu and Y.-F. Zhou, Phys. Rev. D **71**, 021701 (2005).
- [10] M. Gronau, Phys. Lett. B **627**, 82 (2005); M. Gronau and J. L. Rosner, Phys. Rev. D **59**, 113002 (1999); H. J. Lipkin, Phys. Lett. B **445**, 403 (1999).
- [11] B. Aubert *et al.* [BABAR Collaboration], Phys. Rev. Lett. **94**, 181802 (2005), B. Aubert *et al.* [BABAR Collaboration], Phys. Rev. Lett. **95**, 151803 (2005), B. Aubert *et al.* [BABAR Collaboration], Phys. Rev. Lett. **93**, 131801 (2004).
- [12] B. Aubert *et al.* [BABAR Collaboration], Nucl. Instrum. Methods Phys. Res. A **479**, 1 (2002).
- [13] B. Aubert *et al.* [BABAR Collaboration], Phys. Rev. D **66**, 032003 (2002).
- [14] S. Eidelman *et al.* [Particle Data Group], Phys. Lett. B **592**, 1 (2004).
- [15] M. Pivk and F. R. Le Diberder, Nucl. Instrum. Meth. A **555**, 356 (2005).
- [16] B. Aubert *et al.* [BABAR Collaboration], hep-ex/0508046.

- [17] J. Charles *et al.* [CKMfitter Group], Eur. Phys. J. C **41**, 1 (2005).
- [18] B. Aubert *et al.* [BABAR Collaboration], hep-ex/0607098; B. Aubert *et al.* [BABAR Collaboration], hep-ex/0607097; B. Aubert *et al.* [BABAR Collaboration], hep-ex/0607092, submitted to Phys. Rev. Lett.; B. Aubert *et al.* [BABAR Collaboration], hep-ex/0608002.
- [19] W. S. Hou, M Nagashima and A. Soddu, Phys. Rev. Lett. **95**, 141601 (2005).

Table 1: Average tagging efficiency  $\epsilon$ , average mistag fraction  $w$ , mistag fraction difference  $\Delta w = w(B^0) - w(\bar{B}^0)$ , and effective tagging efficiency  $Q$  for signal events in each tagging category. The quantities are measured in the  $B_{\text{flav}}$  sample.

Category	$\epsilon$ (%)			$w$ (%)			$\Delta w$ (%)			$Q$ (%)		
Lepton	8.67	$\pm$	0.08	3.0	$\pm$	0.3	-0.2	$\pm$	0.6	7.7	$\pm$	0.1
Kaon I	11.0	$\pm$	0.08	5.3	$\pm$	0.4	-0.6	$\pm$	0.7	8.7	$\pm$	0.2
Kaon II	17.2	$\pm$	0.1	15.5	$\pm$	0.4	-0.4	$\pm$	0.7	8.2	$\pm$	0.2
Kaon Pion	13.8	$\pm$	0.09	23.5	$\pm$	0.5	-2.4	$\pm$	0.8	3.9	$\pm$	0.1
Pion	14.4	$\pm$	0.09	33.0	$\pm$	0.5	5.2	$\pm$	0.8	1.7	$\pm$	0.1
Inclusive	9.6	$\pm$	0.08	41.9	$\pm$	0.6	4.6	$\pm$	0.9	0.25	$\pm$	0.04
Untagged	23.4	$\pm$	0.12									
Total $Q$										30.4	$\pm$	0.3

Table 2: The results for the  $B^0 \rightarrow \pi^0\pi^0$  and  $B^\pm \rightarrow h^\pm\pi^0$  decay modes are summarized. For each mode, the number of signal events  $N_S$ , total detection efficiency  $\varepsilon$ , branching fraction  $\mathcal{B}$ , and  $CP$  asymmetry are given. Errors on  $\mathcal{B}$  and the asymmetries are statistical and systematic, respectively, while errors for  $N_S$  are statistical and those for  $\varepsilon$  are purely systematic.

Mode	$N_S$	$\varepsilon$ (%)	$\mathcal{B}(10^{-6})$	Asymmetry
$B^0 \rightarrow \pi^0\pi^0$	$140 \pm 25$	$27.1 \pm 1.7$	$1.48 \pm 0.26 \pm 0.12$	$C_{\pi^0\pi^0} = -0.33 \pm 0.36 \pm 0.08$
$B^\pm \rightarrow \pi^\pm\pi^0$	$572 \pm 53$	$32.1 \pm 1.8$	$5.12 \pm 0.47 \pm 0.29$	$\mathcal{A}_{\pi\pi^0} = -0.019 \pm 0.088 \pm 0.014$
$B^\pm \rightarrow K^\pm\pi^0$	$1239 \pm 52$	$26.8 \pm 1.3$	$13.3 \pm 0.56 \pm 0.64$	$\mathcal{A}_{K\pi^0} = 0.016 \pm 0.041 \pm 0.012$

Table 3: Systematic uncertainties in the determination of the  $B^0 \rightarrow \pi^0\pi^0$  branching fraction (left) as a percentage change, and the  $C_{\pi^0\pi^0}$  asymmetry (right) as an absolute change.

Source	$\Delta\mathcal{B}(\pi^0\pi^0)$	Source	$\Delta(C_{\pi^0\pi^0})$
$\pi^0$ efficiency	6.0%	tagging	0.06
$\Delta E$ resolution	3.6%	$m_{\text{ES}}$ and $\Delta E$	0.04
$m_{\text{ES}}$ PDF endpoint	3.1%	$B$ background asymmetry	0.03
mean of $\Delta E$ and $m_{\text{ES}}$	1.9%	Total	0.08
$\mathcal{B}(B \rightarrow \rho\pi)$	1.8%		
luminosity	1.1%		
Total	8.2%		

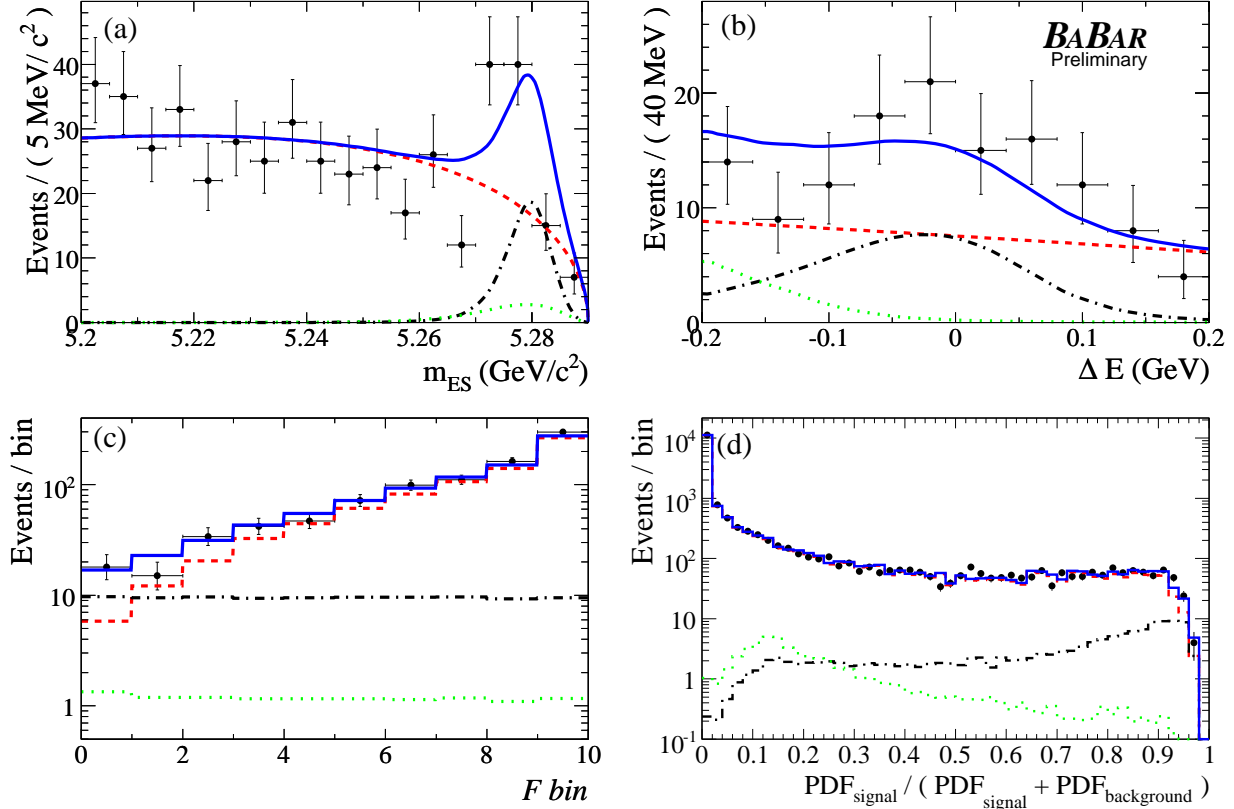


Figure 1: The distributions of (a)  $m_{\text{ES}}$ , (b)  $\Delta E$ , and (c) Fisher discriminant  $\mathcal{F}$  for  $B^0 \rightarrow \pi^0 \pi^0$  candidates that satisfy an optimized requirement on the signal probability, based on all variables except the one being plotted. The projections contain 27%, 30% and 68% of the signal, 20%, 21% and 23% of the  $\rho\pi^0$  background, and 2.8%, 0.047% and 4.8% of the continuum background, for  $m_{\text{ES}}$ ,  $\Delta E$ , and  $\mathcal{F}$ , respectively. The PDF projections are shown as a dashed line for  $q\bar{q}$  background, a dotted line for  $B^\pm \rightarrow \rho^\pm \pi^0$  and  $B^0 \rightarrow K^0 \pi^0$ , and a dashed-dotted line for  $B^0 \rightarrow \pi^0 \pi^0$  signal. The solid line shows the sum of all PDF projections. The PDF projections are scaled by the expected fraction of events passing the probability-ratio requirement. Also shown (d) is the ratio of the PDF for signal to the PDF for signal plus background comparing data (points) to the components of the PDF model.

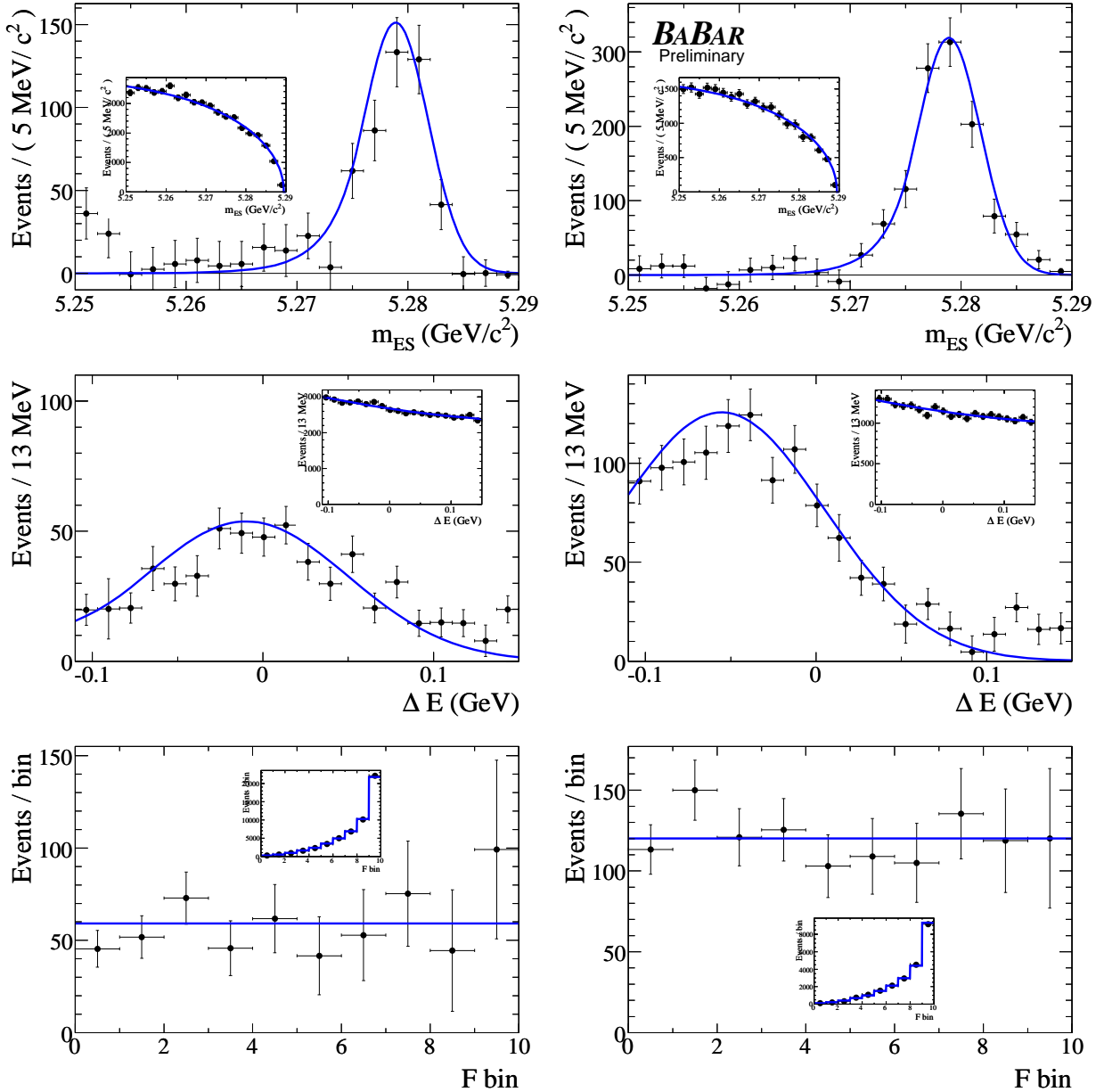


Figure 2: The distributions and PDF projections of  $m_{ES}$  (top),  $\Delta E$  (middle), and Fisher discriminant  $\mathcal{F}$  (bottom), for  $B^\pm \rightarrow \pi^\pm \pi^0$  (left) and  $B^\pm \rightarrow K^\pm \pi^0$  (right) candidates. The main plots show the signal data (points) and PDF (line) after event weighting and background subtraction with the method described in [15]; the method uses all variables except the one being plotted. The insets show the corresponding distributions for background.

Table 4: Dominant systematic uncertainties for  $B^\pm \rightarrow \pi^\pm\pi^0$  and  $B^\pm \rightarrow K^\pm\pi^0$ , as percentage changes in the branching fractions  $\mathcal{B}$  (left), and absolute changes in the asymmetries  $\mathcal{A}_{\pi^\pm\pi^0}$ ,  $\mathcal{A}_{K^\pm\pi^0}$  (right).  $\mathcal{A} = (N_{B^0} - N_{\bar{B}^0}) / (N_{B^0} + N_{\bar{B}^0})$ .

Source	$\Delta\mathcal{B}(\pi^\pm\pi^0)$	$\Delta\mathcal{B}(K^\pm\pi^0)$	Source	$\Delta(\mathcal{A}_{\pi\pi^0})$	$\Delta(\mathcal{A}_{K\pi^0})$
$m_{\text{ES}}$ and $\Delta E$ res.	3.1%	2.4%	$m_{\text{ES}}$ and $\Delta E$	0.007	0.003
$\mathcal{F}$ PDF	3.1%	2.1%	$B$ background	0.009	0.002
$\pi^0$ efficiency	3.0%	3.0%	detector asymmetry	0.008	0.011
$\Delta E$ mean	1.2%	3.0%	Total	0.014	0.012
fit bias	1.1%	1.8%			
$B$ background	0.7%	0.2%			
$h^\pm$ identification	0.7%	0.8%			
Total	5.6%	4.8%			

Table 5: The results for the  $B^0 \rightarrow h^+h^-$  decay modes are summarized. For each mode, the number of signal events  $N_S$  and  $CP$  asymmetries are shown. Errors are statistical and systematic.

Mode	$N_S$	Asymmetry
$B^0 \rightarrow \pi^+\pi^-$	$675 \pm 42$	$S_{\pi\pi} = -0.53 \pm 0.14 \pm 0.02; C_{\pi\pi} = -0.16 \pm 0.11 \pm 0.03$
$B^0 \rightarrow K^+\pi^-$	$2542 \pm 67$	$\mathcal{A}_{K\pi} = -0.108 \pm 0.024 \pm 0.008$
$B^0 \rightarrow K^+K^-$	$11 \pm 19$	—

Table 6: Summary of systematic uncertainties on  $\mathcal{A}_{K\pi}$ ,  $S_{\pi\pi}$ , and  $C_{\pi\pi}$ . The total uncertainty is calculated as the sum in quadrature of the individual contributions.

Source	$\mathcal{A}_{K\pi}$	$S_{\pi\pi}$	$C_{\pi\pi}$
PDF parameters	0.0007	0.0003	0.0011
Tagging/Vertexing	—	0.0178	0.0170
SVT alignment	—	0.0100	0.0022
Beam spot	—	0.0100	0.0100
Tag-side interference	—	0.0080	0.0230
$\tau_{B^0}$ and $\Delta m_d$	—	0.0015	0.0036
Potential bias	0.0078	0.0051	0.0036
Total	0.0078	0.0247	0.0300

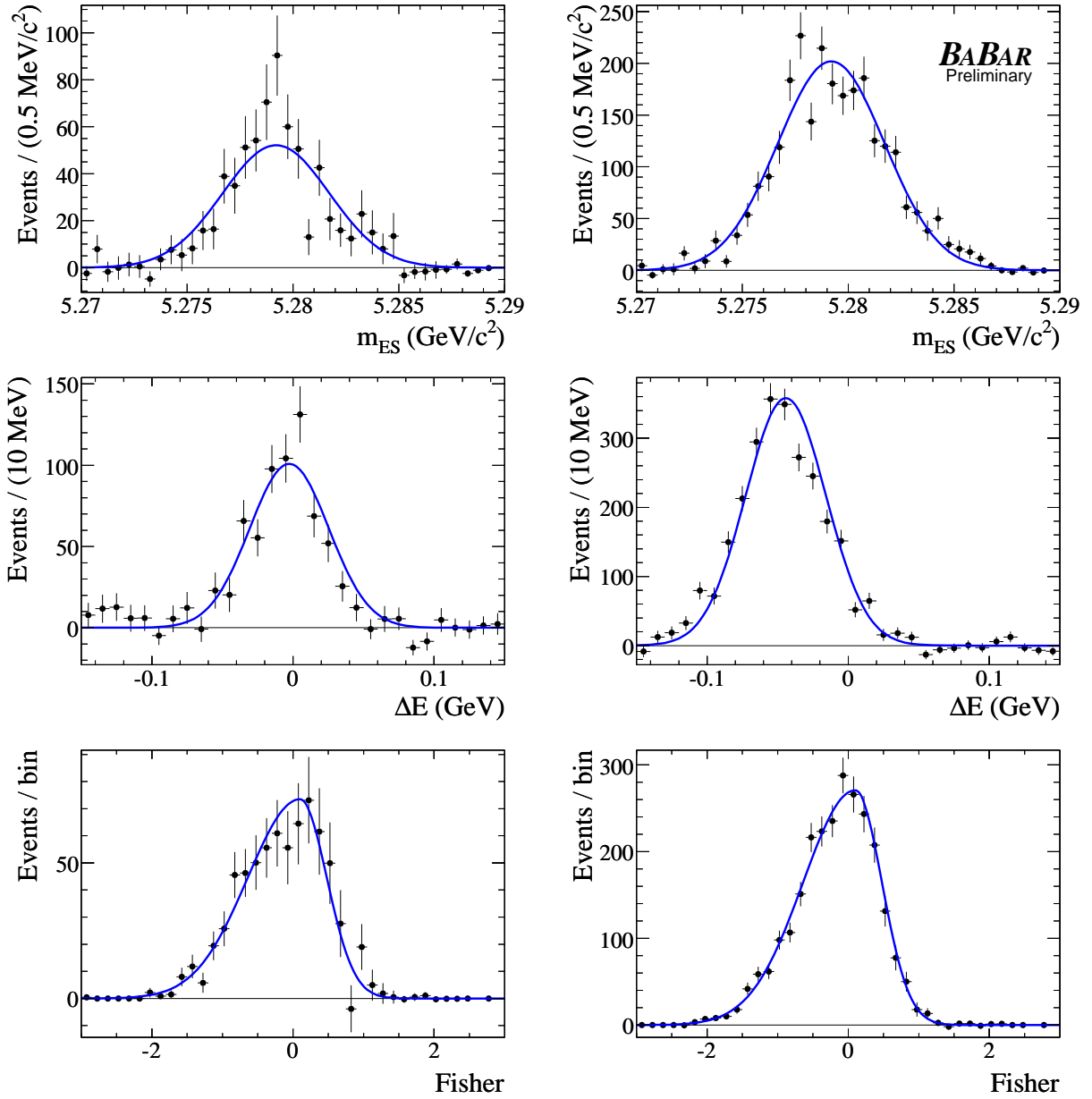


Figure 3: The background-subtracted distributions of  $m_{\text{ES}}$  (top),  $\Delta E$  (middle), and Fisher discriminant  $\mathcal{F}$  (bottom) for signal  $B^0 \rightarrow \pi^+\pi^-$  (left) and  $B^0 \rightarrow K^+\pi^-$  (right) candidates in the data. The curves represent the PDFs used in the fit.

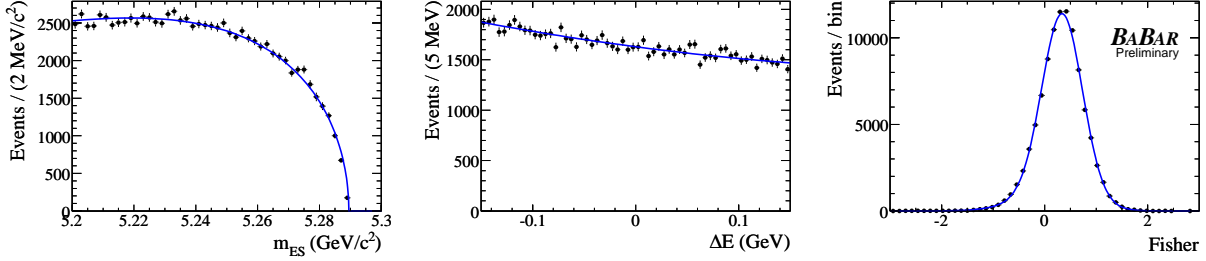


Figure 4: The signal-subtracted distributions of  $m_{\text{ES}}$  (left),  $\Delta E$  (middle), and Fisher discriminant  $\mathcal{F}$  (right) for all background  $h^+h^-$  candidates in the data. The curves represent the PDFs used in the fit.

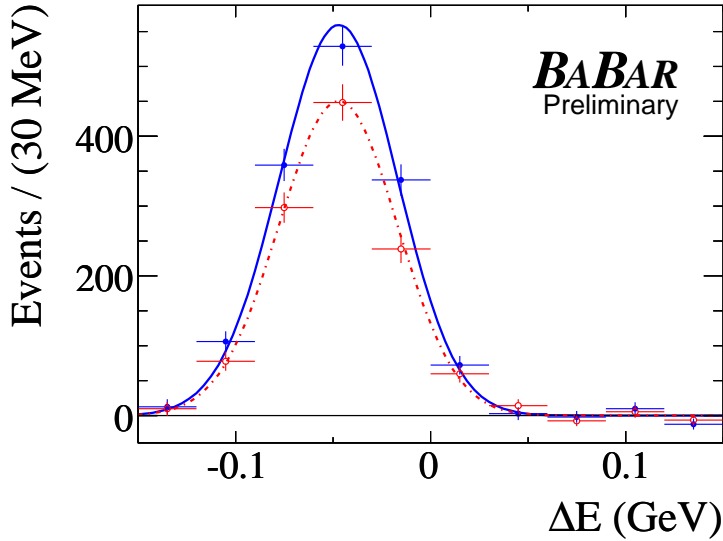


Figure 5: The background-subtracted distribution of  $\Delta E$  for signal  $K^\pm\pi^\mp$  events, comparing  $B^0$  (solid) and  $\bar{B}^0$  decays (dashed).

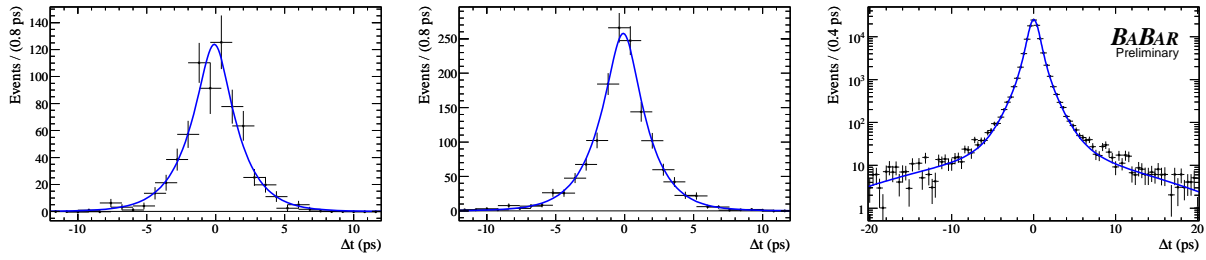


Figure 6: The background-subtracted distributions of  $\Delta t$  for signal  $\pi^+\pi^-$  (left),  $K^\pm\pi^\mp$  (middle), and the signal-subtracted  $\Delta t$  distribution for background candidates in the data (right). The curves represent the PDFs used in the fit.

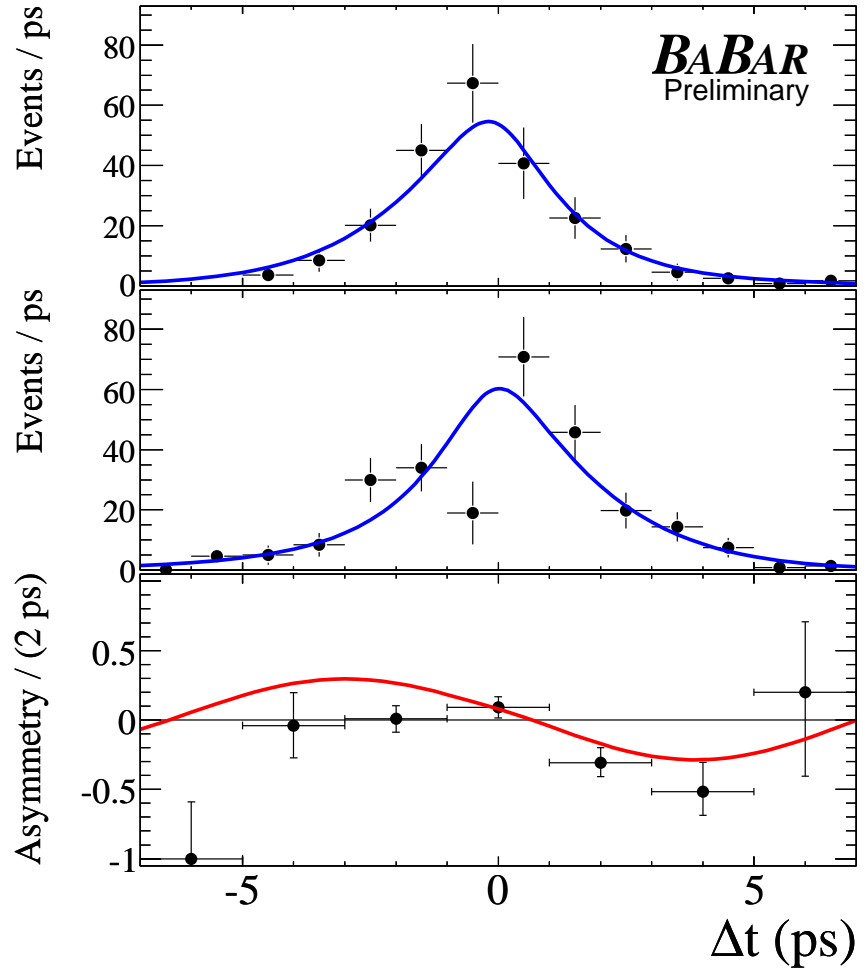


Figure 7: The background-subtracted distributions of  $\Delta t$  for signal  $\pi^+\pi^-$  events tagged as  $B^0$  (top) or  $\bar{B}^0$  (middle), and the asymmetry, defined as  $\mathcal{A} = (N_{B^0} - N_{\bar{B}^0}) / (N_{B^0} + N_{\bar{B}^0})$  (bottom). The curves represent the PDFs used in the fit.

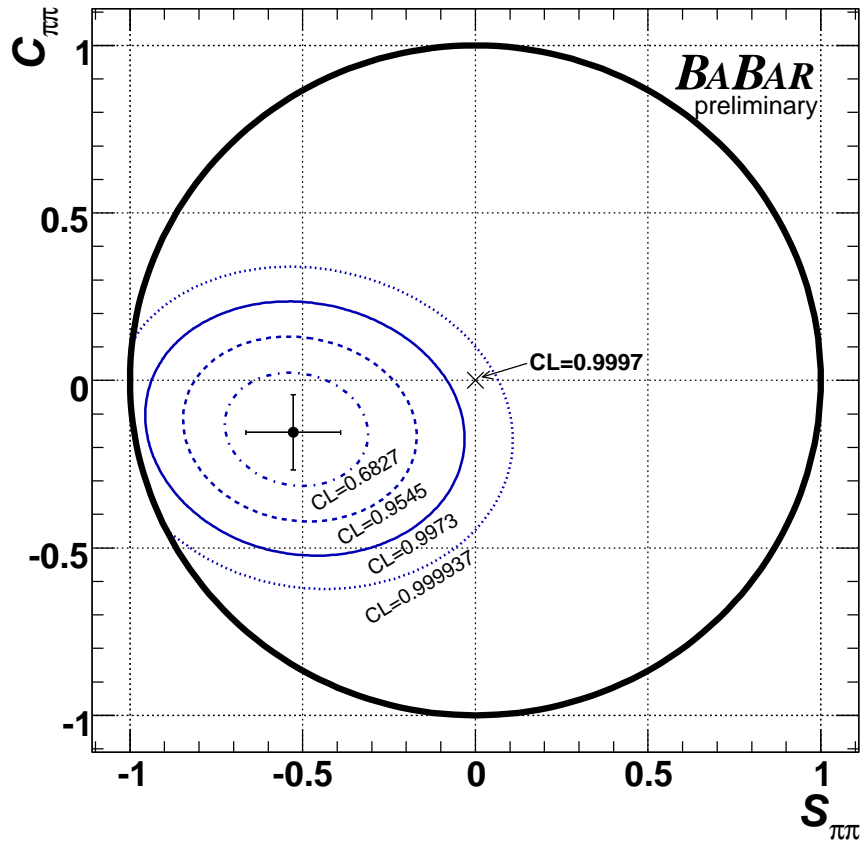


Figure 8: Central value and errors for  $S_{\pi\pi}$  and  $C_{\pi\pi}$  and confidence-level (C.L.) contours. The measured value is  $3.6 \sigma$  from the point of no  $CP$  violation ( $S_{\pi\pi} = 0$ ,  $C_{\pi\pi} = 0$ ), converting from the C.L. to the units of “two-sided” Gaussian significance.

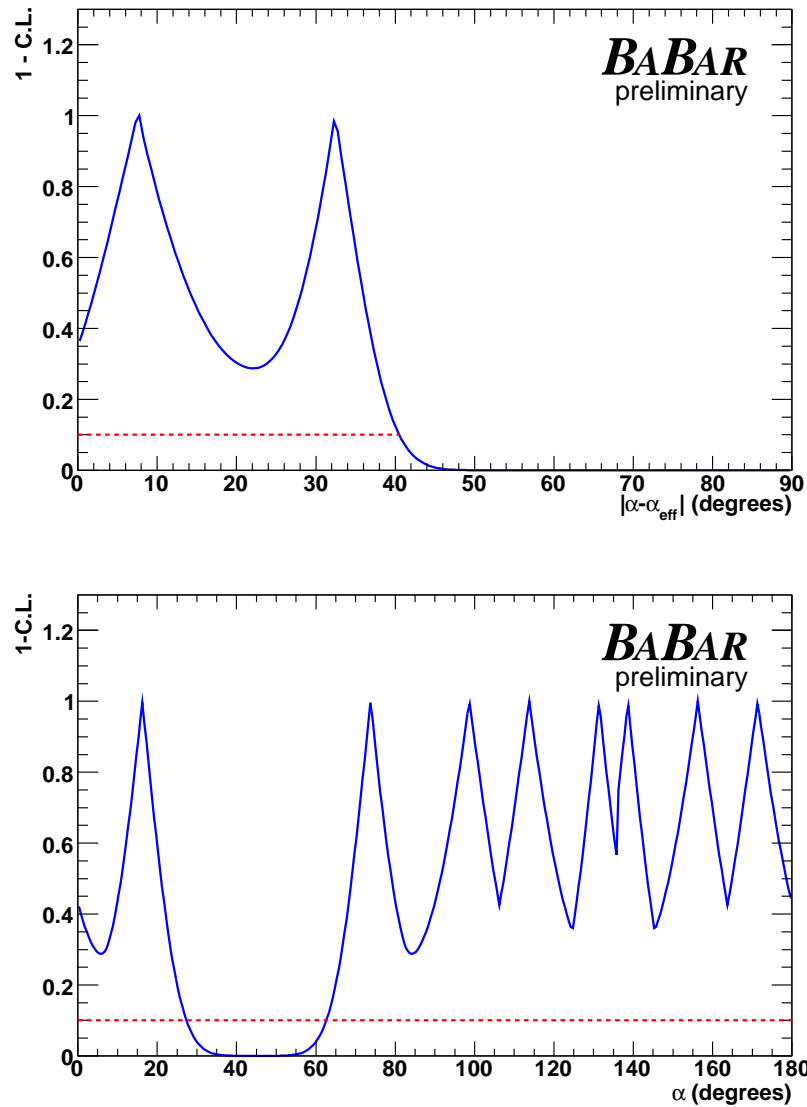


Figure 9: Constraint on the angle  $\Delta\alpha_{\pi\pi} = \alpha - \alpha_{\text{eff}}$  (top), expressed as one minus the confidence level (C.L.) as a function of  $|\Delta\alpha_{\pi\pi}|$ . We find an upper bound on  $|\Delta\alpha_{\pi\pi}|$  of  $41^\circ$  at the 90% C.L. Constraint on the CKM angle  $\alpha$  (bottom) expressed as  $1 - \text{C.L.}$ . The eight peaks correspond to an eight-fold ambiguity in the extraction of  $\alpha$ ; four solutions are from the value and sign of  $\Delta\alpha_{\pi\pi}$ , which is doubled due to the trigonometric reflections between  $\alpha_{\text{eff}}$  and  $\pi/2 - \alpha_{\text{eff}}$ . Only the isospin-triangle relations and the expressions in Eqn. 1 are used in this constraint. The solution at exactly  $\alpha = 0$  is excluded at  $1 - \text{C.L.} = 4.4 \times 10^{-5}$ , not shown in the plot, corresponding to the exclusion of  $S_{\pi\pi} = 0$ ,  $C_{\pi\pi} = 0$  at  $3.6 \sigma$ . Some of the solutions, and the region around  $\alpha = 0$ , can be disfavored by other physics information.